

# Development of a machine vision-based colorimetric system for bell peppers (*Capsicum annuum L.*) using intelligent modelling techniques

Khaled Mohi-Alden\*, Mahmoud Omid\*, Mahmoud Soltani Firouz, Amin Nasiri

(Department of Agricultural Machinery Engineering, Faculty of Agricultural Engineering and Technology, University of Tehran, Karaj 77871-31587, Iran)

**Abstract:** The appearance color of bell peppers is significantly related to their quality which affects consumer's acceptance of buy. Also, homogeneity of color is among the most essential export standards of bell peppers. Commercially standard colorimetric devices are very expensive and are often available in scientific research centers. The aim of the present study was to develop and calibrate a simple, cheap, and portable machine vision (MV)-based system to accurately measure the chromatic parameters of bell peppers. For this purpose, a MV system possessing a digital CCD camera, and an artificial lighting system was developed. To calibrate the color of the utilized camera, the standard color cards were used. An appropriate algorithm based on image processing techniques was developed to calculate the chromatic parameters of the crop in the CIELAB color space. The development system was calibrated and compared with a standard colorimetric device using various developed models including linear regression (LR), multivariate linear regression (MLR), and artificial neural networks (ANNs). All the models were employed to diagnose the chromatic properties of bell peppers using the developed MV system. The results revealed that the LR model outperforms MLR and ANN models. The overall accuracy of the proposed MV system was 91.7% in comparison with the standard device. The results showed that the proposed system can be considered a more reliable device compared to traditional commercial devices and could be a suitable alternative in the absence of a specialized color measurement device.

**Keywords:** bell peppers, colorimetry, CIELAB color space, image processing, machine vision, modelling, calibration

**Citation:** Mohi-Alden, K., M. Omid, M. S. Firouz, and A. Nasiri. 2022. Development of a machine vision-based colorimetric system for bell peppers (*Capsicum annuum L.*) using intelligent modelling techniques. *Agricultural Engineering International: CIGR Journal*, 24 (2):267-281.

## 1 Introduction

The peel color of most agricultural products is an appropriate indicator of their quality level in terms of ripeness level, being healthy or defective, vitreousness and

soundness levels, etc. (Mendoza et al., 2006). Color has been used as an indirect indicator of other quality characteristics of agricultural and food products such as taste and freshness. Quantifying the color properties for agricultural products is one of the first and most important quality characteristics measured in various studies related to the harvesting and postharvest processing. Moreover, color is one of the basic physical attributes on the commercial sorting systems for many agricultural products (Abbott, 1999). Color measurement is an easier method

**Received date:** 2021-01-30 **Accepted date:** 2021-06-28

\*Corresponding author: **Khaled Mohi-Alden and Mahmoud Omid**, Department of Agricultural Machinery Engineering, Faculty of Agricultural Engineering and Technology, University of Tehran, Iran. E-mail: mohialdin@ut.ac.ir, omid@ut.ac.ir. Fax: +98-2632808138.

than chemical tests and is closely related to the physicochemical properties of food and agricultural products (Pathare et al., 2013). The color coordinates are measured using different color spaces such as RGB, CIELAB, HSV, and XYZ. In the RGB color space, the color is comprised of three components including red ( $R$ ), green ( $G$ ), and blue ( $B$ ). Similarly, the color in other color spaces is composed of different components including  $L^*$ ,  $a^*$ ,  $b^*$ ,  $H$ ,  $S$ , etc. (Gonzalez et al., 2009). Most of commercially standard colorimetric instrumentations determine the values of color components based on the CIE LAB color space such as Micromatch Plus (P&K et al., 2010) and spectrophotometer devices (Bayramoglu et al., 2020; Hojabri et al., 2021).

The spectrophotometric instruments measure the distribution of the spectrum when reflected or transmitted through the sample (Pathare et al., 2013). The term “image processing” is used to describe the processing of images taken by a digital camera or a scanner. In general, an image can be described by two variables function  $f(x, y)$ , where  $x$  and  $y$  are spatial coordinates. When the values of  $x$ ,  $y$ , and  $f$  in an image are finite, distinct, and discrete, this image is called a digital image (Gonzalez et al., 2009). The digital image is made up of very small square points, each having a special color. When these points are placed side by side, they form an image. These points are called pixels. The number of pixels in an image defines the image size. Digital images can be processed using these pixels and converting them into a matrix. Each element of the matrix is equal to a corresponding pixel in the digital image (Pound and French, 2014).

The numerical value of each pixel represents the amount of light emitted from the object and received by the camera. In binary images, the numerical value of each pixel is 0 or 1; a pixel with no light (full black) is given a score of 0 and the one with full brightness (white) receives 1 (Pound and French, 2014). In general, the machine vision (MV) system consists of three main parts: image acquisition, image processing, and image analysis (Timmermans, 1995). Today, the MV technique has been

widely adopted in various medical, defense, and agricultural sectors. Applications of this technology in food industries and postharvest processing for agricultural crops include quality detection, grading, food packaging, etc. (Baigvand et al., 2015; Nasiri et al., 2019; Omid et al., 2019).

Bell pepper (*Capsicum annuum L.*) is the third most important crop of the *Solanaceae* family after tomato and potato (Patel et al., 2019). Depending on this plant's variety, bell pepper is found in three different colors, including green, yellow, and red. Generally, the initial color of all mature bell peppers is green. Green bell peppers turn into red or other colors when they are completely ripe. Homogeneity of color are among the most significant export standards of bell peppers. It is also of note that the fully ripen bell peppers with a color ratio less than 70% are not favored by consumers. So, conducting a colorimetry test for bell peppers in the field would be very important to prepare the high-quality crop in packaging the export purposes. Also, measuring the chromatic properties of bell peppers is very significant test for investigation from the effect of post-harvest treatments on the crop quality (i.e., storage, packaging, etc.). Unfortunately, commercially available standard colorimetric instruments are very expensive. Therefore, its use is currently limited to laboratory applications in scientific research centers and universities.

Recently, a computer vision system (CVS) was developed to measure the color of milks and milk products. The obtained results were compared with a commercial colorimeter. Although the accomplished test showed that there was the difference between color measured by the CVS and the colorimeter device (colorimeter readings resulted in a darker and yellower color based on average  $L^*a^*b^*$  values, while CVS readings resulted in lighter and less yellow appearance), but it was indicated that the CVS is reliable for measurement the color and should be considered as a superior tool for replacing traditional devices by offering improved representativeness and accuracy (Milovanovic et al.,

2021).

In a similar study, two methods of color measurement; including a developed CVS and a traditional colorimeter, were compared for color evaluation of meat products. CVS color was more laborious to obtain, but was more accurate and representative, especially for non-uniformly colored samples (Tomasević et al., 2019).

However, standard colorimetric devices usually calculate the color components values at local zones of the products. Therefore, the calculated color values (despite calculating the average value of several points) are not representative to the colorimetric characteristics of the whole fruit, especially for such products that have a large color difference on their surfaces such as immature bell peppers. Accordingly, this study aims to develop a simple, cheap, and portable system as an alternative to commercial instruments, based on MV technique for measuring the chromatic parameters of bell peppers.

## 2 Material and methods

In this research, a MV-based colorimetric system with all its appropriate components (hardware and software) to measure the chromatic parameters of bell peppers was developed. Then, the developed system was calibrated and evaluated with a standard colorimetric device using three different modelling techniques including linear regression (LR), multivariate linear regression (MLR), and artificial neural networks (ANNs).

### 2.1 Imaging system

The body of the imaging system was fabricated from a wooden cube with dimensions of 500 mm × 400 mm × 500 mm. For uniformity in brightness intensity and reducing the effects of reflection of light, the inner surfaces of the box were painted black. A platform to put the product sample was placed at a height of 200 mm in the middle of the base. To improve the image quality, the platform was covered with black cloth. Samples can be easily inserted inside the imaging chamber through the opening door of the box. A circular hole was created at the top of the box, and a digital CCD camera (Ace1300-200uc, Basler

company, Germany) was mounted inside the hole at 300 mm away from the platform. The lighting system consists of two LED lamps (models 4014LED 18 Watt, 12 V DC, 100 cm, China). The main advantages of this lamp are low heat generation, the ability to use both types of currents (AC and DC), and its persistent brightness over time. To have an evenly distributed light of the LED lamps, the LED strips were placed inside special protective covers (LED Profile, China) made of aluminum. To achieve a uniform lighting conditions, four 0.25m sections of the lamps were placed in a square form at the middle of the top inside the box and two 50 cm strips were placed on the sides.

To prevent light intensity reduction of the lamps due to the decrease in the amount of voltage (Crowell, 2000), all parts of the lamps were connected in parallel with the selected power supply (an adapter or a battery). The minimum amount of current required for this configuration 3A. Because the imaging box was designed to be used in the laboratory during this study, an adapter (HS-12040, China) was added to the lighting system to convert the input voltage from AC to DC. The adapter was selected according to the required current for the lighting of the lamps, whose input is 100-240V and 1.5A (AC), and its output is 12 V and 4A (DC). To use the proposed device in the agricultural land as a portable device, just a 12V lead-acid battery is sufficient to power the lighting system (i.e., model 6-FM-3.5, 12V 3.5 AH, 1.3 kg, Yangtze Solar company, China). To calibrate the amount of light inside the box and minimize the effects of light reflection caused by high brightness, an LED-intensity adjuster or dimmer (model RVNI, 12 volts, China) was used. In the dimmer used in this study, the light intensity inside the box can be adjusted by a remote controller. After turning on the camera, the appropriate light intensity inside the box was determined experimentally to provide a good noise-free image. This dimmer can save light intensity settings. For this reason, and to achieve the same lighting conditions, the selected light intensity in the dimmer was kept constant during device evaluation.

To capture the images, first, the sample is placed on the platform. Then, to reduce noise and to prevent the interference of natural light and creating shadows, the door of the imaging box is closed and the images are taken using the CCD camera. All images of the product samples must be taken from a constant distance as well as under the same lighting conditions. Also, the camera settings must be the same so as the color specifications of the acquired images would be correctly compared. The utilized camera

works through special software (*pylon viewer* software, Basler company, Germany) installed on the PC. In this software, by clicking on the capture button, the images are stored directly into the PC. The software recognizes all camera settings such as brightness, contrast, and focus. The PC, which is the core of the MV system, processes all the acquired digital images by an appropriate algorithm. The main components of the fabricated MV system are shown in Figure 1.

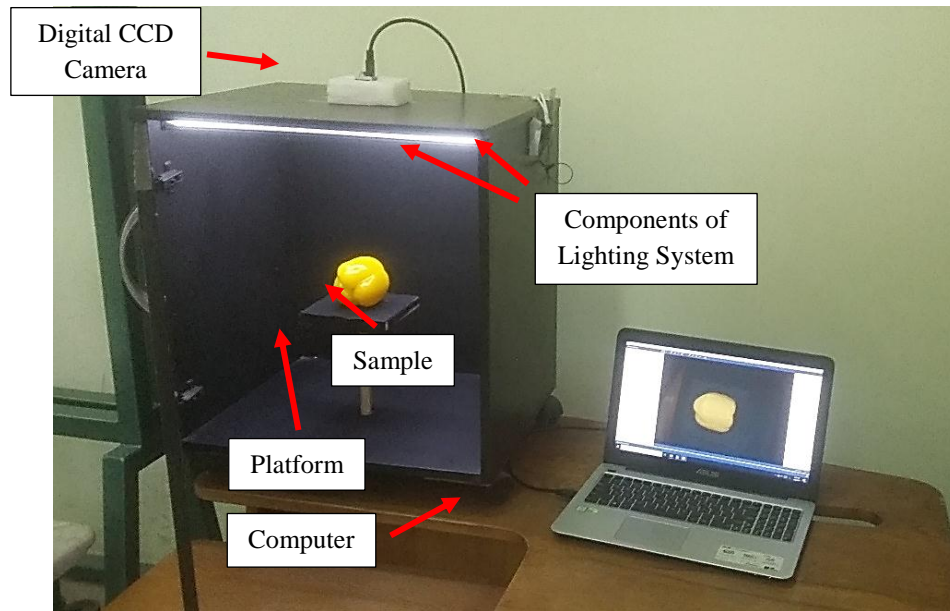


Figure 1 The developed MV system

**2.2 Camera color calibration**

At the pre-test step, three different cameras were examined including a mobile phone camera (Model: Samsung Galaxy Grand Prime, G530F) and two digital CCD cameras (Model: Microsoft Life Cam studio TM, China; Model: Ace1300-200uc, Basler company, Germany). However, since each camera provides different color component values, it is necessary to calibrate the camera utilized. For this purpose, a color card consisting of 24 color patches was used (Anonymous, 2021) and printed with high resolution on an A3 size paper (Figure 2). Next, the average values of color components ( $L^*$ ,  $a^*$ , and  $b^*$ ) for each color patch were obtained and calculated using a standard colorimetric device (Model: Chroma Meter CR-400, Konica Minolta company, Japan).

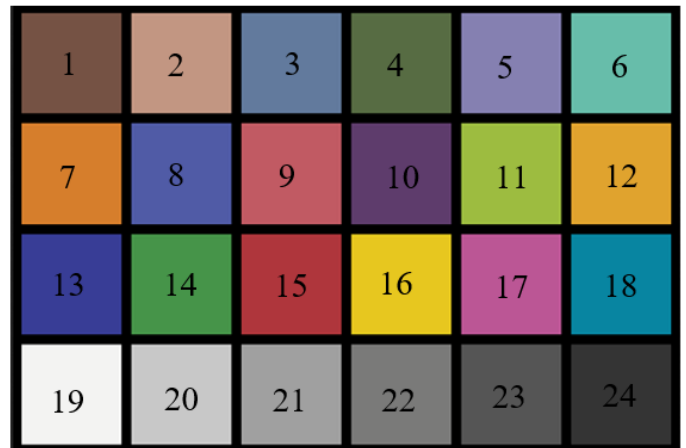


Figure 2 The utilized color card numbered from 1 to 24

To calibrate the color of the used camera, the color card was placed on the platform inside the imaging box and an image was captured for all the color patches. The acquired color card image was stored on the PC. Using *Microsoft Office Picture Manager* Software, each color

patch was cropped and stored as an individual image. Next, the average color values of components  $R$ ,  $G$ , and  $B$  of each color patch image were extracted using the *mean* function in MATLAB. Afterward, the average values of color components  $L^*$ ,  $a^*$ , and  $b^*$  were obtained using an image processing algorithm. Next, the correlations between standard color components (actual value) and the measured color components (predicted values) were obtained by peer-to-peer comparison of the average color values computed using the standard colorimetric device with the average values obtained from our proposed system. Finally, in order to calibrate the utilized camera, three different models including LR, MLR, and ANNs models were developed. To examine the accuracy of each model in diagnose of the peel color of bell peppers, the obtained relationships related to each model were added later to the developed algorithm to modify the predicted values of the color components in the proposed MV device.

### 2.2.1 LR and MLR models

In the LR model, the correlation between each standard color components ( $L^*$ ,  $a^*$ , or  $b^*$ ) and the associated measured color components ( $L_0^*$ ,  $a_0^*$ , or  $b_0^*$ ) were investigated. To obtain the best correlation, linear relation and quadratic polynomial relations were tested.

On the other hand, to investigate the correlation between each standard color components ( $L^*$ ,  $a^*$ , or  $b^*$ ) and all the measured color components in CIELAB color space ( $L_0^*$ ,  $a_0^*$ , and  $b_0^*$ ), three relationships were obtained using MLR. For that, different MLR models types including interactions, pure quadratic, and quadratic values for independent variables were examined.

### 2.2.2 ANN model

To predict the standard (actual) color values of the used color chart based on the color values measured using the MV system, MLP ANNs with three-layers (Figure 3) were designed. The ANNs were designed with three neurons in input layer (CIE Lab color values measured by MV system) and three neurons in output layer (CIE Lab color values obtained by Minolta). The trial and error

method was used in order to obtain the best network structure. In this research, just one hidden layer was studied and the various ANN models associated with different number of neurons in the hidden layer (from 1 to 20 neurons) were examined. In all cases, the transfer functions for the neurons in the hidden layer were selected as hyperbolic tangent (tansig) and the activation function for the output layer was selected as linear (purelin). Also, Levenberg-Marquardt (LM) backpropagation and gradient descent with momentum (GDM) algorithms were employed to train the networks. Generally, the ANNs require a large dataset for its optimization in order to get its benefit of generalization and nonlinear mapping. However, the number of data available was 25 data. To overcome this obstacle, the developed MLP networks were trained through 10-fold cross-validation method. For that, the training dataset was divided randomly into 10 subsets. A single subset was utilized for validation of the network, while the other nine subsets were used for training the model. This cross-validation process was repeated for 10 times. In each training time, the validation set was shifted from one fold to another. In all developed models, 70% of the dataset were selected as training data and 30% of the dataset were selected as testing data.

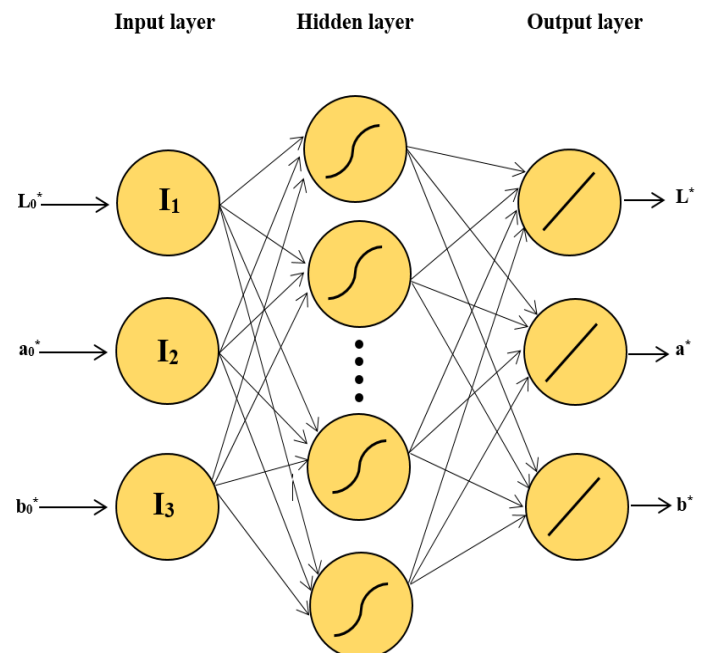


Figure 3 The structure of the developed MLP ANNs

The best regression correlation equations and the optimum ANN model were selected based on the values of root mean square error (*RMSE*) and coefficient of determination ( $R^2$ ) indicators. *RMSE* and  $R^2$  are given by Omid et al. (2009):

$$RMSE = \sqrt{\frac{\sum_{i=1}^n (O_i - P_i)^2}{n}} \quad (1)$$

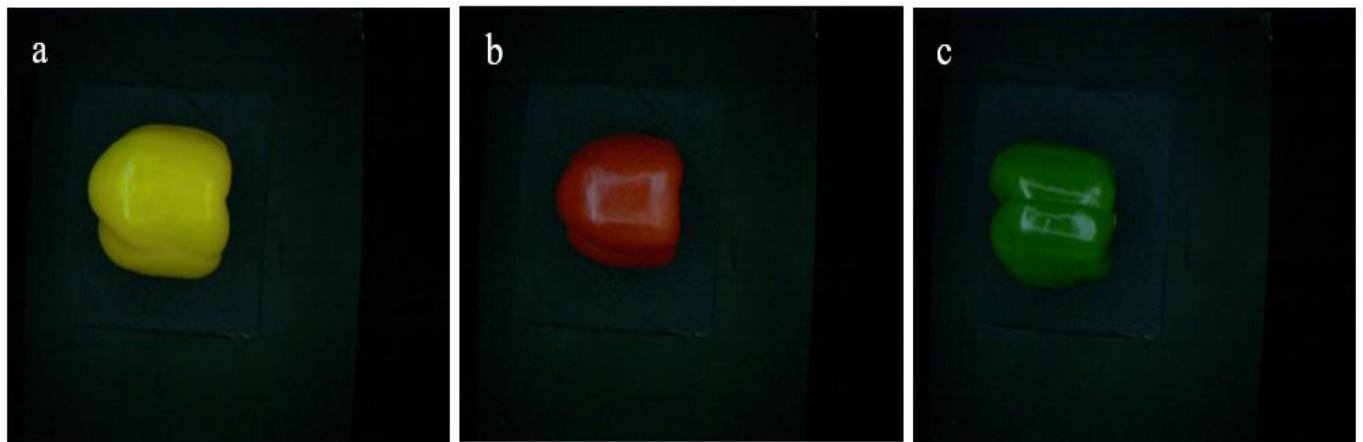
$$R^2 = 1 - \frac{\sum_{i=1}^n (O_i - P_i)^2}{\sum_{i=1}^n (O_i - \bar{O}_i)^2} \quad (2)$$

where  $O_i$  represent the actual value,  $P_i$  is the estimated value,  $n$  is the number of data and  $\bar{O}_i$  represent the average of actual values.

**2.3 Sample preparation and image acquisition**

For evaluating the developed MV-based colorimetric system, a total of 27 fresh bell peppers (*Capsicum annuum L.*) at three maturity levels including full green, full red,

and full yellow (nine samples at each maturity stages) were prepared in January 2021 from a local market in Karaj city, Iran (latitude 35 °49' 50.271"N, longitude 50 °56' 6.094"E, altitude 1280 m). The samples were transferred immediately to the laboratory of physical properties in department of mechanical engineering of biosystem, university of Tehran, Karaj, Iran (latitude 35 °47' 57.784"N, longitude 50 °59' 44.964"E, altitude 1333 m). At the same day, all samples were placed at 20 °C and 75% ± 5% RH on a clean table. Afterward, the surface of the specimens was manually cleaned using a soft and humid cloth. To take the images, the bell peppers were horizontally placed one after the other inside the developed MV system on the platform under the camera. Then, the images of bell peppers at all different maturity levels (Figure 4) were acquired and directly transferred and saved on the PC using the USB 3.0 port of the camera for subsequent analysis. The images were saved in high resolution with RGB color space, 1280×1024 pixel size, and 24 bit depth.



(a) full yellow bell pepper, (b) full red bell pepper, and (c) full green bell pepper

Figure 4 Acquired images of bell peppers in three different maturity levels

**2.4 Developed image processing algorithm**

In the alternative colorimetric device, computer algorithms were developed to process the taken images of the product sample and extract the average values of the color components ( $L^*$ ,  $a^*$ , and  $b^*$ ) from the surface of the bell pepper sample. The main steps of the image processing algorithms embedded in the proposed device

are illustrated in Figure 5. Initially, the images were acquired from the bell pepper samples. Then, using an appropriate algorithm, the images were segmented and the bell peppers were isolated from the background. In the next step, pixel coordinates of the bell peppers were extracted and the color features of the pixels were obtained.

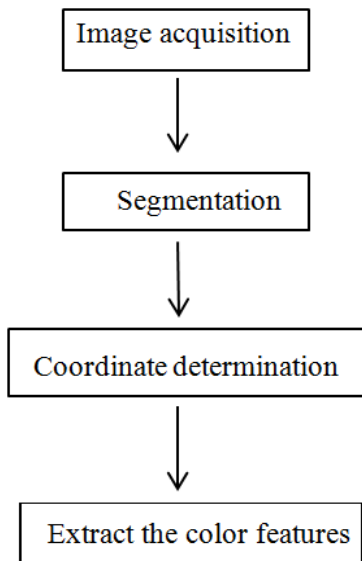
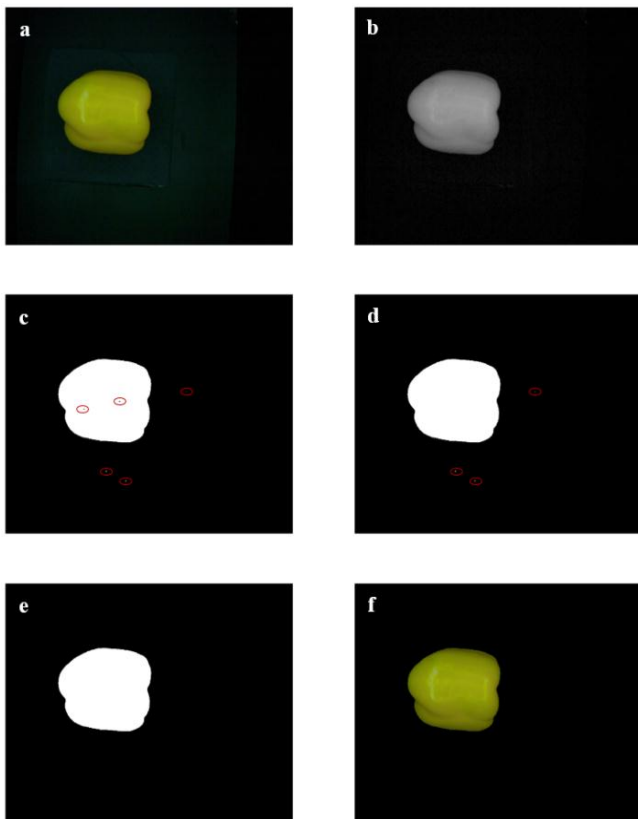


Figure 5 The main steps of the image processing algorithms



(a) Original image, (b) R-component of bell pepper image, (c) Primary binary image obtained from Otsu method, (d) Secondary binary image after filling the white holes, (e) Final binary image after applying the morphological operator, and (f) Segmented image obtained by multiplying the final binary image in the original RGB image

Figure 6 Segmentation steps of the captured yellow bell pepper using Otsu's thresholding method in the red channel of RGB color space

#### 2.4.1 Image segmentation

Image segmentation is one of the most challenging tasks in image processing techniques. This is a critical step in the image processing algorithms because extracting the desired features in the next steps highly relies on the success of this step. Since, the acquired images of the bell peppers had high qualities and were noise-free, no preprocessing was necessary to improve their qualities. In the present study, segmentation was performed to isolate the bell pepper samples from the background. In the literature, Otsu's thresholding method (Otsu, 1979) has been suggested for the segmentation of agricultural and food products (Teimouri et al., 2018; Mohi-Alden et al., 2019). Otsu's method is one of the best automatic thresholding methods. So, Otsu's thresholding method was employed to separate the bell peppers from background. Experiments on various bell pepper samples with different colors and by examining different channels of several color spaces, revealed that the red color channel ( $R$ ) of the RGB color space has a high contrast between a bell pepper and background (Figure 6b). Accordingly, the  $R$  component in RGB color space was selected to transform the RGB image of the bell peppers into the primary binary image type (Figure 6c). However, in the obtained binary image, there are some noise or holes (small black points) on the white object area produced due to the reflection of light in some points on the peel of the bell pepper. Moreover, some white points on the black background are seen due to the presence of some dust and small paint points on the background of the imaging system. So, it is necessary to delete these noises before subsequent analyses. The black holes (zero values) in the previous image were filled and converted to white holes using MATLAB's *imfill* function (Figure 6d). Then, morphological operations were employed to remove the second noise. In the second binary image (Figure 6d), MATLAB's *bwareaopen* function was applied to remove all jointed components (objects) that have pixels count less than a certain limit. In other words, objects with more area than a certain limit (in this study, 150 pixels) was retained.

This function was used for enhancing diagnostic accuracy. As a result, the pixel count of the objects in the resulted image will be more than 150. In the output binary image, just one object (bell pepper sample) remained. The white points (equal to one) in the final binary image refer to the bell pepper sample (Figure 6e). In the next step, the segmented image was obtained by multiplying the final binary image (Figure 6e) in the original RGB image (Figure 6a). The segmented image is shown in Figure 6f.

2.4.2 Coordinate determination

The purpose of this step is to calculate the average color of pixels forming the bell pepper. On the segmented image, MATLAB’s *reshape* function and MATLAB’s *find* function were applied to extract the coordinates of those pixels (Gonzalez et al., 2009). *Reshape* function sorts the color pixels in rows *I*. Then, the *find* function finds the rows whose pixels are not black. These were the same pixels that form the bell pepper sample. These pixels were stored as a triple column matrix.

2.4.3 Extraction of the color features

In the generated triple column matrix, the average of each color component (*R*, *G*, and *B*) was obtained using MATLAB’s *mean* function. Then, the three-stage method was used to move from RGB color space to CIELAB color space (Aghilinategh et al., 2016). For this purpose, initially, the non-linear RGB values were converted to the linear sRGB values using Equation 3 and Equation 4, as long as the values of *R*, *G*, and *B* are greater than 0.04045 (Anderson et al., 1996):

$$sR = (R + 0.055 / 1.055)^{2.4}$$

$$sB = (B + 0.055 / 1.055)^{2.4} \tag{3}$$

Otherwise:

$$sR = (R / 12.92)$$

$$sG = (G / 12.92) \tag{4}$$

$$sB = (B / 12.92)$$

After that, the values of xyz color space components are obtained from sRGB values calculated using the following coefficient matrix.

$$\begin{bmatrix} x \\ y \\ z \end{bmatrix} = \begin{bmatrix} 0.4124 & 0.3576 & 0.1805 \\ 0.2126 & 0.7152 & 0.0722 \\ 0.0193 & 0.1192 & 0.9505 \end{bmatrix} \times \begin{bmatrix} sR \\ sG \\ sB \end{bmatrix} \tag{5}$$

In the final stage, the components of xyz are transformed into CIELAB color space components using Equation 6 (CIE, 1986):

$$L^* = [116 \times \text{var}(y)] - 16$$

$$a^* = 500 \times [\text{var}(x) - \text{var}(y)] \tag{6}$$

$$b^* = 200 \times [\text{var}(y) - \text{var}(z)]$$

To this end, the values of var (*x*), var (*y*) and var (*z*) are calculated using Equation 7 and Equation (8). As long as

the values of these ratios ( $\frac{x}{x_n}$ ,  $\frac{y}{y_n}$ , and  $\frac{z}{z_n}$ ) are greater than 0.008856:

$$\text{var}(x) = \left(\frac{x}{x_n}\right)^{\frac{1}{3}}$$

$$\text{var}(y) = \left(\frac{y}{y_n}\right)^{\frac{1}{3}} \tag{7}$$

$$\text{var}(z) = \left(\frac{z}{z_n}\right)^{\frac{1}{3}}$$

Otherwise:

$$\text{var}(x) = [7.787 \times \left(\frac{x}{x_n}\right)] + \frac{1}{16}$$

$$\text{var}(y) = [7.787 \times \left(\frac{y}{y_n}\right)] + \frac{1}{16} \tag{8}$$

$$\text{var}(z) = [7.787 \times \left(\frac{z}{z_n}\right)] + \frac{1}{16}$$

where *x<sub>n</sub>*, *y<sub>n</sub>* and *z<sub>n</sub>* represent the *x*, *y*, and *z* values in standard reference of white color at D<sub>65</sub> illumination (i.e., 95.047, 100, and 108.883, respectively).

All steps of image processing methodology were carried out in *MATLAB 2018a* software using the image processing toolbox. Also, all the developed LR, MLR, and ANNs models were designed by *MATLAB*. To work with all software used in this research and to implement all algorithms, a laptop with the following specifications was

used: Intel Core i7-6500u, 3.1 GHz, 8 GB RAM, Windows 10 Pro 64 Bit.

### 3 Results and discussion

#### 3.1 Camera calibration

Table 1 presents the actual average values of the color components in the CIELAB color space obtained using the utilized standard Minolta device for 24 patches related to the utilized color card according to their numbers in the color card (see Figure 2).

To calibrate the camera used in the developed MV system, first, the average values of each color patch in the RGB color space were extracted using the developed image processing algorithm. After that, the three-stage method described above was employed to move from RGB color space to CIELAB color space. Table 2 presents the average values of the color components  $R$ ,  $G$ ,  $B$ ,  $L^*$ ,  $a^*$ , and

$b^*$  obtained using the proposed colorimetric device for all twenty-four patches.

##### 3.1.1 Linear regression model

Based on the values obtained for the color components, significant correlations were established between the standard color values (actual values) and the measured (predicted values) ones in CIELAB related to the 24 patches of the color card. The equations representing the relationship between the standard and the measured values of CIELAB color components are given in Table 3. Results of linear regression (LR) analysis showed polynomial relations between  $L^*/L_0^*$  and  $a^*/a_0^*$  components. Meanwhile, a linear relation was obtained between components  $b^*$  and  $b_0^*$ . The results showed a good correlation between the standard and the measured values of the CIELAB color components.

**Table 1 Average values for the 24 color card patches in the CIELAB color space**

No.	$L^*$	$a^*$	$b^*$
1	38.91	5.98	9.06
2	61.61	9.96	17
3	43.04	-0.76	-18.4
4	38.97	-9.71	9.76
5	51	4.78	-23.65
6	49.85	-18.4	-12.98
7	46.85	18.68	49.94
8	41.79	4.21	-35.24
9	52.3	25.2	20.49
10	36.25	13.53	-9.98
11	60.81	-23.39	35.55
12	72.63	7.37	58.34
13	38.08	10.21	-37.92
14	42.82	-25.49	14.11
15	44.3	27.33	22.12
16	77.59	-2.92	62.74
17	49.67	32.74	13.96
18	37.94	-10.14	-17.47
19	84.13	2	8.34
20	68.2	0.41	2.72
21	44.41	-0.7	1.95
22	46.27	-1.34	2.94
23	37.98	-0.4	3.07
24	31.94	-0.99	2.2

Note:  $L^*$ ,  $a^*$ , and  $b^*$  are the average standard values of the color components.

**Table 2 Average measured color values of the 24 color card patches in the RGB and CIELAB color spaces**

No.	$R_0$	$G_0$	$B_0$	$L_0^*$	$a_0^*$	$b_0^*$
1	102.28	91.83	79.82	39.65	2.03	8.45
2	146.52	124.56	104.28	53.73	5.21	14.21
3	71.2	104.99	130.14	42.86	-4.96	-17.75
4	55.18	72.96	36.34	28.66	-14.49	19.62
5	94.89	110.94	156.15	47.22	5.85	-26.39
6	73.49	136.03	128.42	52.53	-22.13	-2.19
7	173.73	131	50.4	57.5	8.18	48.17
8	32.23	76.47	153.92	33.72	13.96	-46.65
9	147.69	101.11	87.98	47.37	17.07	15
10	59.65	32.81	82.37	21.49	23.43	-25.15
11	119.18	154.19	13.79	59.1	-29.85	59.69
12	188.71	158.69	33.05	66.2	-1	63.39
13	65.09	86.13	155.33	38.17	13.6	-40.29
14	56.77	109.48	49.02	41.41	-30.67	28.14
15	135.64	87.65	73.87	42.18	18.13	16.17
16	174.47	160.53	26.23	65.32	-8.54	63.95
17	138.15	76.1	100.63	40.46	29.38	-2.7
18	62.81	107.2	116.91	42.6	-12.5	-10.2
19	154.01	166.06	155.23	66.93	-6.35	4.14
20	132.47	140.52	132.82	57.6	-4.47	3.09
21	79.64	90.35	81.81	37.24	-6.07	3.52
22	76.54	86.92	78.14	35.82	-6.03	3.72
23	71.38	85.35	78	34.92	-7.15	2.46
24	73.37	83.85	74.79	34.51	-6.17	3.91

Note:  $R_0, G_0, B_0, L_0^*, a_0^*$ , and  $b_0^*$  are the average values of the measured color components.

**Table 3 Correlation relationship between the standard and measured values of CIELAB color components using the LR model**

Color component	Correlation relationship
$L^*$	$L^* = 0.0221L_0^{*2} - 1.0244L_0^* + 47.403$
$a^*$	$a^* = -0.0029a_0^{*2} + 0.8792a_0^* + 4.345$
$b^*$	$b^* = 0.8476b_0^* + 0.7962$

Note:  $L_0^*, a_0^*$  and  $b_0^*$  are the average values of the measured color components. Also,  $L^*, a^*$ , and  $b^*$  are the average standard values of the color components.

3.1.2 Multivariate linear regression model

Results of MLR analysis showed a good relation between Minolta color values and color components values predicted by MV system. The best performance for

prediction of  $L^*$  and  $a^*$  values were obtained using pure quadratic MLR relations. While, a quadratic MLR relation was extracted to estimate  $b^*$  value. The correlation equations for these parameters are presented in Table 4.

**Table 4 Correlation relationship between the standard and measured values of CIELAB color components using the MLR model**

Color Component	Correlation relationship
$L^*$	$L^* = 50.727 - 1.314L_0^* + 0.08a_0^{*2} - 0.036b_0^* + 0.027L_0^{*2} + 0.003a_0^{*2} - 0.001b_0^{*2}$
$a^*$	$a^* = -21.646 + 1.227L_0^* + 1.019a_0^* + 0.195b_0^* - 0.014L_0^{*2} - 0.004a_0^{*2} - 0.001b_0^{*2}$
$b^*$	$b^* = 15.229 - 0.719L_0^* - 0.195a_0^* + 0.315b_0^* + 0.015L_0^*a_0^* + 0.013L_0^*b_0^* - 0.002a_0^*b_0^* + 0.009L_0^{*2} + 0.002a_0^{*2} - 0.005b_0^{*2}$

Note:  $L_0^*, a_0^*$  and  $b_0^*$  are the average values of the measured color components. Also,  $L^*, a^*$ , and  $b^*$  are the average standard values of the color components.

3.1.3 ANN model

The topology of the optimal ANN model (i.e., 3-4-3) developed here is illustrated in Figure 7. The performance of the developed MLP networks using different numbers

of neurons in the hidden layer is shown in Figure 8. According to this diagram, we can evaluate and compare the accuracy of this model with others. Based on the analysis and the comparison of the  $R^2$  and  $RMSE$  related to

training and testing dataset for various MLP structures, the best ANN model had four neurons in the hidden layer (as shown in Figure 7). This model had the lowest *RMSE* and

the highest  $R^2$  values during network training and testing. The results obtained from this model are presented in Table 5.

**Table 5 Results related to the optimal ANN model**

Network topology	Performance ( $R^2$ )		Error		Training algorithm	Error function	Hidden activation	Output activation
	Train	Test	Train	Test				
MLP 3-4-3	98.06%	94.02%	4.09	7.1	Back-propagation	<i>RMSE</i>	Tan-sigmoid	Linear

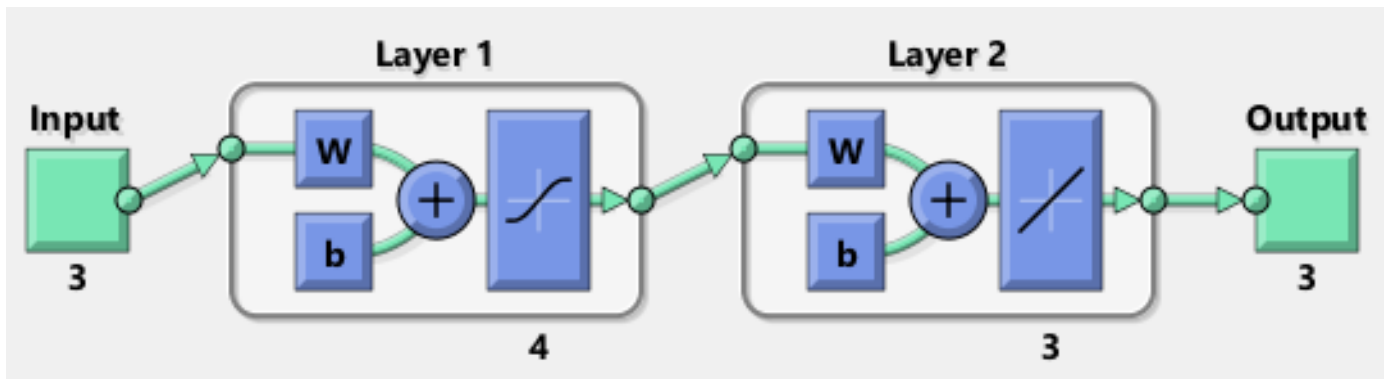


Figure 7 The optimal ANN model with mlp-3-4-3 structure for predicting the color component values

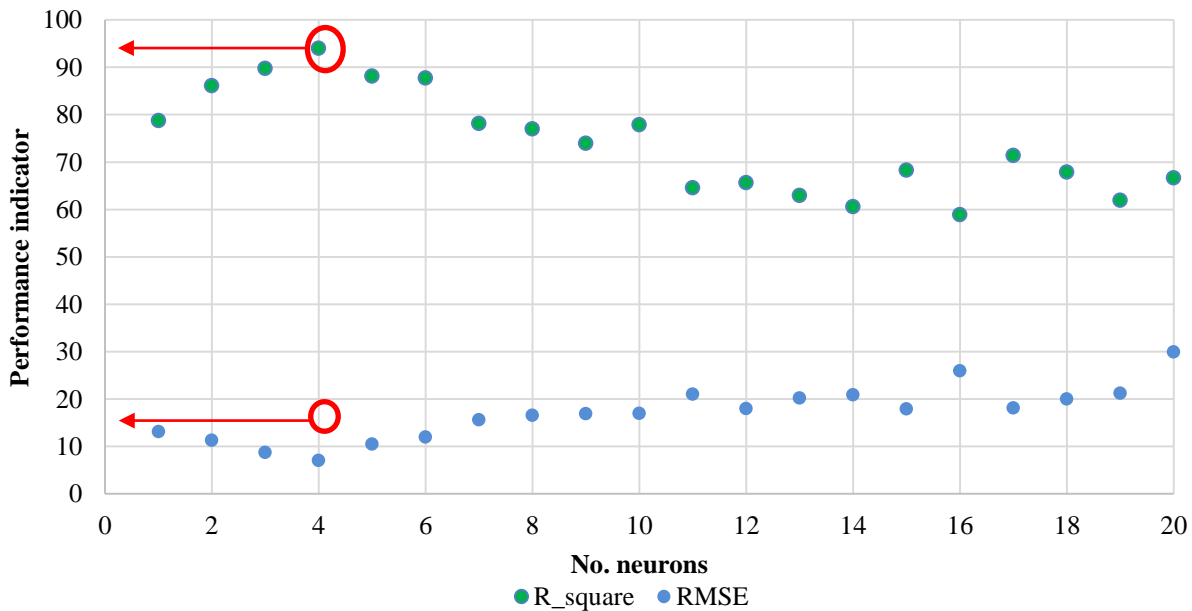


Figure 8 The accuracy results of the developed ANNs related to testing dataset

### 3.2 MV system evaluation

The developed system was evaluated for measuring the chromatic properties of red, green, and yellow bell peppers. Based on the obtained results, the color component values of the peel of this crop in the CIELAB color space were obtained using both the standard Minolta device and the designed MV system. All the developed models (i.e., LR, MLR, and ANN) were employed in order

to correct the color values of bell peppers obtained using the proposed MV system. The results of correlation as  $R^2$  and *RMSE* between the actual color values obtained using Minolta and the predicted color values calculated using MV system for each model were compared. The  $R^2$  values for the LR, MLR, and ANN models were 91.71%, 86.08%, and 82.91%, respectively. While, The *RMSE* amounts for the LR, MLR, and ANN models were 7.38, 9.87, and

11.56, respectively. It can be concluded that the LR model had the highest  $R^2$  and the lowest  $RMSE$  values comparing to MLR and ANN models. The probable reason for better output of LR model than ANN model is the over-fitting problem that may happen due to little the number of data. Generally, LR models have less parameters to estimate than ANN models for a same set of input variables. So, the LR model showed better adjusted even though the number of data was not large. Based on that, the LR model was

selected to be used in the proposed MV system. For that, the obtained correlation equations related to the LR model (Listed in Table 3) were added to the developed image processing algorithms in order to correct the measured color values of bell peppers. The results of correlation between the actual color values obtained using Minolta and the predicted color values calculated using MV system for the selected LR model is shown in Figure 9.

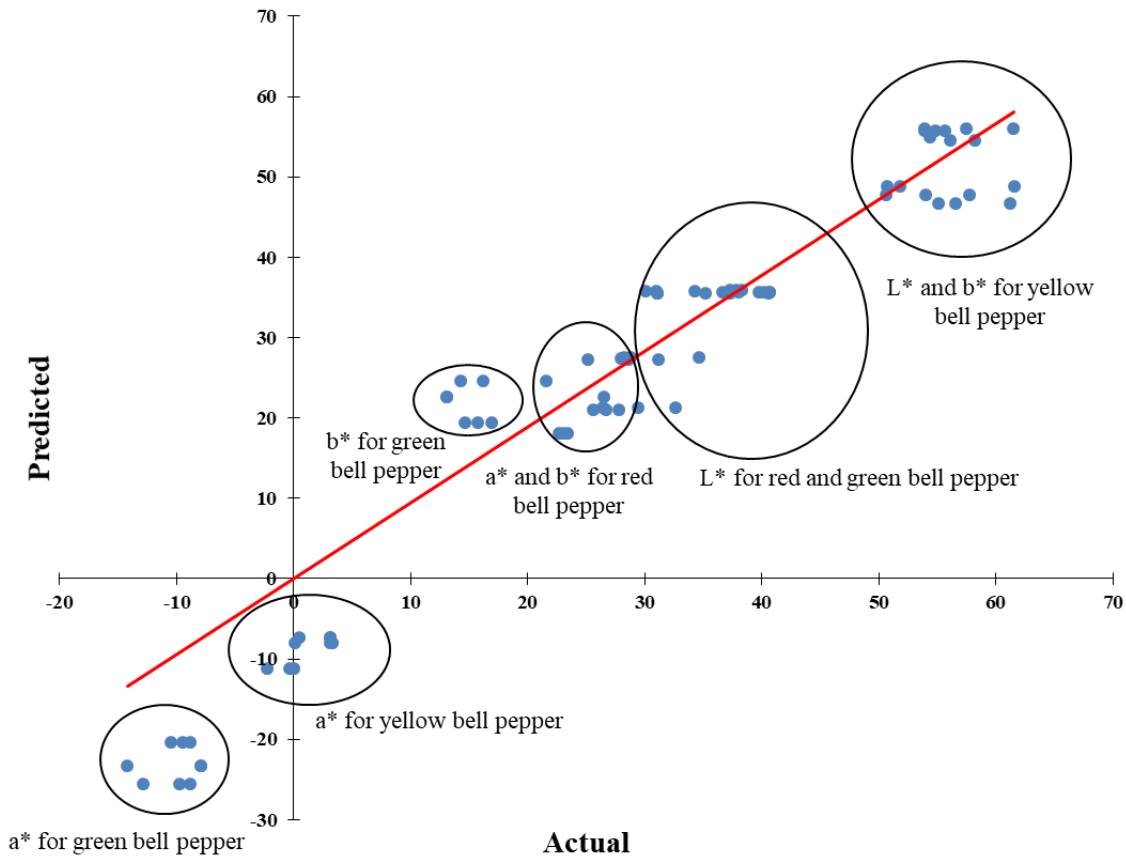


Figure 9 Correlation between actual and predicted values of  $L^*$ ,  $a^*$ , and  $b^*$  color components for colored bell peppers

As shown in Figure 9, the  $L^*$  values for all colored bell peppers,  $a^*$  and  $b^*$  for red bell peppers, and  $b^*$  for yellow bell pepper were predicted with a high accuracy by the proposed MV system. Also, it is seen that the data groups of these parameters are located on the baseline in regression correlation between actual color values measured by the Minolta device and predicted values calculated by the developed MV system (Figure 9). Meanwhile, the  $b^*$  values for green bell peppers was acceptably estimated using the developed device. As

shown in Figure 9, the obtained data for these groups are close to the baseline. In comparison,  $a^*$  values for yellow bell peppers and  $a^*$  value for green bell pepper is not predicted by the proposed colorimetric device, well. Totally, the  $a^*$  component is relative to the green-red opponent colors. The range of  $a^*$  component is -127 to +127 with negative values toward green and positive values toward red. From the estimation of  $a^*$  for yellow bell pepper, it can be concluded that the positive prediction of  $a^*$  component values was fairly good. Meanwhile, the

more we go toward the negative values of this component, the more the prediction power gets worse. This error may be explained by the reflection of light that occurs on the outer glossy appearance of bell peppers, especially green peppers that have negative values for the  $a^*$  component. This result, which is denoted by white color in the acquired images (see Figure 4c), led to the error in

calculating the average color for the outer surface of the sample. However, the total prediction accuracy of the proposed system was obtained as 91.71%. Figure 10 presents a comparison between the color obtained using Minolta and the proposed MV system. It is clear how the predicted color by MV system is very close to the actual one.

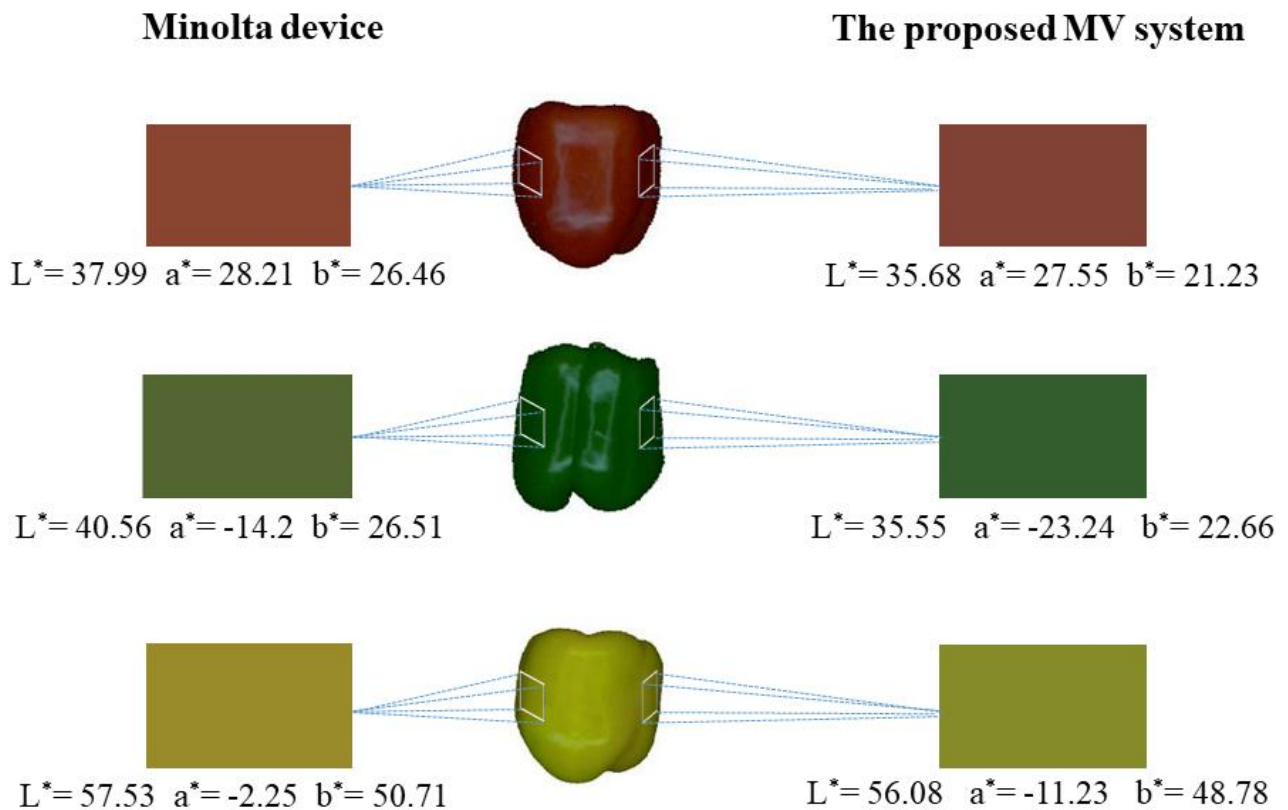


Figure 10 Comparison between the color obtained using Minolta and the MV proposed system

These results show that the designed system could be a suitable alternative for measuring the chromatic parameters of bell peppers in the absence of a specialized color measurement device. Furthermore, the proposed system is suitable as a portable colorimetric device for use at a fixed place in food industry laboratories or in the agricultural lands.

#### 4 Conclusion

In the present study, a simple, cheap, and portable colorimetric system was developed based on machine vision (MV) to measure the chromatic properties of bell peppers. Generally, the commercially standard colorimetric devices measure the chromatic parameters

just in CIE LAB color space. While, the proposed system can calculate more color components (i.e.,  $R, G, B, x, y, z, L^*, a^*$ , and  $b^*$ ) of the crop directly. Also, the developed MV system has the ability to compute the chromatic properties of the total surface of the crop. While, standard colorimetric devices such as Minolta compute the color components values at local points of the products. Hence, the proposed MV-based colorimetric system can be considered as a more reliable device compared to traditional commercial devices. For future research, to improve the accuracy of the system, some modifications on the utilized lighting system would be beneficial. For example, different types of light sources would be examined. Also, the order of the lightening system inside

the box can be changed and evaluated. Furthermore, because the lamps in this study were installed horizontally on the ceiling of the box, the arrangement of the lamps with special angles may reduce the light reflection of the sample surface.

## Acknowledgments

This research was supported by University of Tehran (UT). We would like to thank UT for financing this project.

## References

- Abbott, J. A. 1999. Quality measurement of fruits and vegetables. *Postharvest Biology and Technology*, 15(3): 207-225.
- Aghilinategh, N., S. Rafiee, S. Hosseinpour, M. Omid, and S. S. Mohtasebi. 2016. Real-time color change monitoring of apple slices using image processing during intermittent microwave convective drying. *Food Science and Technology International*, 22(7): 634-646.
- Anderson, M., R. Motta, S. Chandrasekar, and M. Stokes. 1996, January. Proposal for a standard default color space for the internet—srgb. In *Color and Imaging Conference*, 1: 238-245. Scottsdale, Arizona, USA, November 19-22, 1996.
- Anonymous, 2021. Wikipedia Macbeth chart RGB values. Available at: <https://www.dpreview.com/forums/post/58686976>. Accessed 17 March 2021.
- Baigvand, M., A. Banakar, S. Minaei, J. Khodaei, and N. Behroozi-Khazaei. 2015. Machine vision system for grading of dried figs. *Computers and Electronics in Agriculture*, 119(10): 158-165.
- Bayramoglu, E. E., F. C. Topuz, M. M. Ayana, and S. Soyly. 2020. A Research on the use of waste mandarin peels as fixing agents in leather production and its effects on ageing and colour. *Turkish Journal of Agriculture-Food Science and Technology*, 8(2): 266-269.
- Crowell, B. 2000. *Electricity and Magnetism*. 2nd ed. Fullerton, California, USA: Light and Matter.
- Hojabari, N., D. Kaisarly, and K. H. Kunzelmann. 2021. Adhesion and whitening effects of P11-4 self-assembling peptide and HAP suspension on bovine enamel. *Clinical Oral Investigations*, 25(5): 3237-3247.
- Gonzalez, R. C., R. E. Woods, and E. L. Eddins. 2009. *Digital Image Processing Using MATLAB*. 2nd ed. USA: Gatesmark Publisher.
- Mendoza, F., P. Dejmek, and J. M. Aguilera. 2006. Calibrated color measurements of agricultural foods using image analysis. *Postharvest Biology and Technology*, 41(3): 285-295.
- Mohi-Alden, K., M. Omid, A. Rajabipour, B. Tajeddin, and M. S. Firouz. 2019. Quality and shelf-life prediction of cauliflower under modified atmosphere packaging by using artificial neural networks and image processing. *Computers and Electronics in Agriculture*, 163(8): 104861.
- Milovanovic, B., V. Tomovic, I. Djekic, J. Miocinovic, B. G. Solowiej, J. M. Lorenzo, F. J. Barba, and I. Tomasevic. 2021. Colour assessment of milk and milk products using computer vision system and colorimeter. *International Dairy Journal*, 120(9): 105084.
- Nasiri, A., A. Taheri-Garavand, and Y. D. Zhang. 2019. Image-based deep learning automated sorting of date fruit. *Postharvest Biology and Technology*, 153(7): 133-141.
- Omid, M., A. Baharlooei, and H. Ahmadi. 2009. Modeling drying kinetics of pistachio nuts with multilayer feed-forward neural network. *Drying Technology*, 27(10): 1069-1077.
- Omid, M., K. Mohi-Alden, and A. Rajabipour. 2019. Using image processing and artificial neural networks to predict quality and shelf-life of cauliflower packaged with MAP technology. In *IVInternational Conference on Theoretical and Applied Computer Science and Engineering*, 1-4. Istanbul, Turkey, October 11-12, 2019.
- Otsu, N. 1979. A threshold selection method from gray-level histograms. *IEEE Transactions on Systems, Man, and Cybernetics*, 9(1): 62-66.
- Pathare, P. B., U. L. Opara, and F. A. J. Al-Said. 2013. Colour measurement and analysis in fresh and processed foods: a review. *Food and Bioprocess Technology*, 6(1): 36-60.
- Patel, N., S. Gantait, and J. Panigrahi. 2019. Extension of postharvest shelf-life in green bell pepper (*Capsicum annum* L.) using exogenous application of polyamines (spermidine and putrescine). *Food Chemistry*, 275(6): 681-687.
- P&Z, Z., L. Helyes, and A. Lugasi. 2010. Color changes and antioxidant content of vine and postharvest-ripened tomato fruits. *HortScience*, 45(3): 466-468.
- Pound, M. P., and A. P. French. 2014. An introduction to images and image analysis. In *Plant Image Analysis: Fundamentals and Applications*, eds. S. D Gupta, and Y. Ibaraki, 14-37. Boca Raton, Florida, USA: CRC Press.
- Tomasević, I., V. Tomović, B. Milovanović, J. Lorenzo, V. Đorđević, N. Karabasil, and I. Đekić. 2019. Comparison of a computer vision system vs. traditional colorimeter for color evaluation of meat products with various physical properties. *Meat Science*, 148(2): 5-12.

- Teimouri, N., M. Omid, K. Mollazade, H. Mousazadeh, R. Alimardani, and H. Karstoft. 2018. On-line separation and sorting of chicken portions using a robust vision-based intelligent modelling approach. *Biosystems Engineering*, 167(3): 8-20.
- Timmermans, A. J. M. 1995. Computer vision system for on-line sorting of pot plants based on learning techniques. In *II International Symposium on Sensors in Horticulture, Acta Horticulturae*, 421: 91-98. Tune Landboskole, Greve, Denmark, August 21, 1995.